



Deposited via The University of Leeds.

White Rose Research Online URL for this paper:

<https://eprints.whiterose.ac.uk/id/eprint/160507/>

Version: Accepted Version

Article:

Olanrewaju, FO, Li, H, Andrews, GE et al. (2020) Improved model for the analysis of the Heat Release Rate (HRR) in Compression Ignition (CI) engines. *Journal of the Energy Institute*, 93 (5). pp. 1901-1913. ISSN: 1743-9671

<https://doi.org/10.1016/j.joei.2020.04.005>

© 2020, Elsevier. This manuscript version is made available under the CC-BY-NC-ND 4.0 license <http://creativecommons.org/licenses/by-nc-nd/4.0/>.

Reuse

This article is distributed under the terms of the Creative Commons Attribution-NonCommercial-NoDerivs (CC BY-NC-ND) licence. This licence only allows you to download this work and share it with others as long as you credit the authors, but you can't change the article in any way or use it commercially. More information and the full terms of the licence here: <https://creativecommons.org/licenses/>

Takedown

If you consider content in White Rose Research Online to be in breach of UK law, please notify us by emailing eprints@whiterose.ac.uk including the URL of the record and the reason for the withdrawal request.

Improved Model for the Analysis of the Heat Release Rate (HRR) in Compression Ignition (CI) Engines

Francis O. Olanrewaju^{a,b*}, Hu Li^a, Gordon E. Andrews^a, Herodotos N. Phylaktou^a

^aSchool of Chemical and Process Engineering, Faculty of Engineering and Physical Sciences, University of Leeds, LS2 9JT, United Kingdom

^bDepartment of Engineering Infrastructure, National Agency for Science and Engineering Infrastructure (NASeni), Abuja, Nigeria

Abstract

The accuracy of the Heat Release Rate (HRR) model of Internal Combustion Engines (ICEs) is highly depended on the ratio of specific heats, γ . Previous γ models were largely expressed as functions of temperature only. The effects of the excess air ratio (λ) and the Exhaust Gas Recirculation (EGR) rate on γ were neglected in most of the existing γ functions. Furthermore, previous HRR models were developed for stoichiometric or near – stoichiometric air - fuel mixtures in an engine condition. However, Compression Ignition (CI) engines operate over a wide range of λ . No work has been done to model the HRR of CI engines under non – stoichiometric conditions. Also, no work has been done to investigate the accuracy of existing γ functions specifically with respect to the modelling of the HRR of CI engines for non – stoichiometric conditions. The aim of this work was to develop an improved HRR model for the analysis of the HRR of CI engines for non – stoichiometric conditions ($\lambda > 1$). In this work, a modified $\gamma(T, \lambda)$, was used to model the HRR of a 96 kW, multiple fuel injection, Euro V, Direct Injection (DI) engine. The modified HRR model (Leeds HRR model) predicted the fuel consumption of the engine with an average error of 1.41% confirming that the accuracy of the HRR model of CI engines is improved by using $\gamma(T, \lambda)$. The typical average error in the prediction of the other models was 16%. The much improved HRR model leads to more accurate prediction of fuel consumption, which enables the development of and enhances better fuel consumption management strategies for engines and fuels. It was also ascertained in this work that EGR has insignificant effect on the HRR of CI engines at low and medium loads.

Key words: Combustion, specific heats ratio, excess air ratio, modelling, EGR

* Corresponding author. Tel.: +447503114068; +2347030285759

E-mail address: pmofo@leeds.ac.uk; sonictreasure@gmail.com (F.O. Olanrewaju)

Nomenclature

Symbols:

| | |
|----------|--|
| A_s | Surface area |
| a_i | Coefficients of ratio of specific heats function for unburned mixtures |
| b_1 | Coefficients of ratio of specific heats function for burned mixtures |
| c_m | Mean piston speed |
| c_v | Specific heat capacity at constant volume |
| h | Heat transfer coefficient |
| h_{bb} | Enthalpy of blow - by gases |
| K_1 | Constant |
| m | Amount of gas in cylinder |
| m_{bb} | Mass of blow – by gases |
| m_f | Mass of injected fuel |
| p | Pressure |
| Q | Heat released from injected fuel |
| Q_b | Heat loss through blow – by gases |
| Q_w | Heat loss through cylinder walls |
| q_e | Heat of evaporation of fuel |
| R | Universal gas constant |
| T | Temperature |
| U | Internal energy |
| V | Volume |
| W | Pressure – volume work |

Greek symbols:

| | |
|--------------------------------|--------------------|
| γ | |
| k_1, k_2 | Constants |
| λ | Excess air ratio |
| ϕ | Equivalence ratio |
| ρ | Density |
| θ | Crank Angle Degree |
| $\omega_1, \omega_2, \omega_3$ | Constants |

Subscripts:

| | |
|------|----------------|
| b | Burned mixture |
| bb | Blow – by |

| | |
|------------|------------------|
| <i>e</i> | Evaporation |
| <i>mod</i> | Modified |
| <i>ref</i> | Reference |
| <i>s</i> | Surface |
| <i>u</i> | Unburned mixture |
| <i>w</i> | Wall |

Abbreviations:

| | |
|-----------------|-----------------------------------|
| aTDC | After Top Dead Centre |
| CAD | Crank Angle Degree |
| CHR | Cumulative Heat Release |
| CI | Compression Ignition |
| DI | Direct Injection |
| EGR | Exhaust Gas Recirculation |
| EoC | End of Combustion |
| EVC | Exhaust Valve Closing |
| HRR | Heat Release Rate |
| ICE | Internal Combustion Engine |
| IMEP | Indicated Mean Effective Pressure |
| IVC | Intake Valve Closing |
| MFB | Mass Fraction Burned |
| NO _x | Nitrogen Oxides |
| PHRR | Peak Heat Release Rate |
| rpm | Revolutions per minute |
| SI | Spark Ignition |
| SoC | Start of Combustion |

1. Introduction

Heat Release Rate (HRR) analysis of Internal Combustion Engines (ICEs) is necessary in engine research to carry out analysis of the performance of the engines for pure diesel and renewable/blend fuels engine operation. HRR analysis is also necessary to determine the combustion phasing (Start of Combustion; SoC, End of Combustion; EoC, Peak Heat Release Rate; PHRR) and to enhance the thermal efficiency of the engine. As indispensable as HRR analysis is in engine research, the HRR of an ICE cannot be measured real – time, it can only be modelled mathematically. As such, accuracy is of the essence in the development of HRR models for ICEs. The ratio of specific heats, gamma (γ) is the most important thermodynamic

property in the modelling of the HRR of an ICE [1]. γ has the greatest impact on the accuracy of the HRR model of Internal Combustion Engines (ICEs). The existing models of γ were largely expressed in terms of the temperature of the gases in the cylinder even though γ is known to be strongly dependent on the excess air ratio (λ) of the engine. The EGR rate also has some effect on γ . The existing HRR models were developed for ICEs that were operated at near – stoichiometric conditions ($\lambda \approx 1$). However, Compression Ignition (CI) engines operate within a wide range of λ . Therefore, it is necessary to develop an improved model for the determination of the HRR of CI engines.

In this work, a modified function, $\gamma_{mod}(T, \lambda)$ based on the γ function of Ceviz and Kaymaz [1] was used to model the HRR of a modern, multiple fuel injection, CI engine for values of $\lambda > 1$. The effect of EGR rate on γ was also studied in this work using the improved HRR model. The HRR model of Ceviz and Kaymaz [1] and the improved HRR model in this work (Leeds HRR model) were both based on $\gamma(T, \lambda)$. However, the basic difference between the two models is that, the model of Ceviz and Kaymaz [1] was based on $\gamma(T, \lambda)$ for both burned and unburned fuel mixtures while Leeds HRR model was based on $\gamma(T, \lambda)$ for only burned mixtures (CI engines are lean combustion engines therefore, the fraction of unburned fuel in the exhaust gases is negligible). Secondly, the model of Ceviz and Kaymaz [1] is applicable to SI engines operating at near – stoichiometric conditions while Leeds HRR model is for CI engines at non – stoichiometric conditions.

The improved HRR model in this work was validated by comparing the predicted fuel consumption to the measured fuel consumption. This validation method was used because the fuel consumption of the engine was measured directly by instrumentation, in real – time, during the tests whereas, neither the HRR nor the Cumulative Heat Release (CHR) of an ICE can be measured. In the work of Wu, Keum [2], the heat flux was measured at the wall of the cylinder of a motored engine. The in - cylinder HRR of an engine, as mentioned earlier, can only be modelled mathematically and thereafter, the CHR profile is derived from the modelled HRR. The best method of validating the HRR model of an ICE is to compare a measurable parameter that the HRR is dependent on (such as the fuel consumption) to model prediction. The measured fuel mass was neither used in the modelling of the HRR nor when the fuel consumption was estimated from the modelled HRR/CHR data. For this reason, the measured fuel mass was compared to the predicted masses to validate the Leeds HRR model.

No work has been carried out in the past to model the HRR of a CI engine for non – stoichiometric conditions. Also, no work has been done in the past to investigate the accuracy of existing γ functions for the modelling of the HRR of multiple fuel injection, CI engines operated at non – stoichiometric conditions.

1.1 Effect of fuel injection strategy on the HRR profile of ICEs

Fuel injection in CI engines occurs either by single injection or multiple injection strategy. Fuel injection occurs at a crank angle in a single fuel injection strategy engine. Consequently, the HRR profile of the engine has only one peak as depicted by the lower curve of Figure A.1 [3]. On the other hand, in a multiple injection strategy CI engine, fuel injection occurs at more than one crank angle. Therefore, in contrast to a single injection strategy engine, multiple peaks are observed in the HRR profile of a multiple fuel injection strategy engine as shown in Figure A.2 [4].

Multiple injection strategy is used in modern CI engines to reduce peak pressure, PHRR as well as for emission (NOx) control.

1.2 Previous HRR models

The HRR models in literature differ in terms of the γ functions and the heat transfer coefficient models that the authors used. Various γ models have been proposed in literature ([5], [6], [7], [8], and [9]). Gatowski, Balles [5] used a linear function of the mean charge temperature to model the specific heats ratio. The γ model of the authors was solely a function of temperature (Equation 1).

$$\gamma = \gamma_0 - K_1(T - T_{ref})/1000 \quad (1)$$

The reference value in Equation 1, $\gamma_0 = 1.38$, the constant $K_1 = 0.08$ and the reference temperature, $T_{ref} = 300$ K.

Brunt and Emtage [6] evaluated the HRR of a Spark Ignition (SI) engine by using a second - order function that was derived from a multidimensional model (Equation 2). The γ function in their equation was within a narrow range of λ ($0.83 < \lambda < 1.25$). The γ model was based on the temperature of the gases in the cylinder, T in Kelvin.

$$\gamma = 1.338 - 6.0 \times 10^{-5}T + 1.0 \times 10^{-8}T^2 \quad (2)$$

Egnell [7] proposed an exponential γ function given in Equation 3. The exponential model in Equation 3 is explicitly a function of temperature though the authors chose the values of the constants in the equation based on the combined effects of temperature and gas composition.

$$\gamma = \gamma_0 - k_1 \exp(-k_2/T) \quad (3)$$

The reference value in Equation 3, $\gamma_0 = 1.38$, while the constants k_1 and k_2 have values 0.2 and 900 respectively.

Blair [8] proposed a γ model which is specifically for exhaust gas at stoichiometric condition, equivalence ratio, $\phi = 1$ ($\lambda = 1/\phi = 1$). The model of Blair [8] is also solely depended on temperature as shown in Equation 4.

$$\gamma = 1.4221 - 1.8752e - 4T + 6.9668e - 8T^2 - 9.099e - 12T^3 \quad (4)$$

Ceviz and Kaymaz [1] derived γ functions for unburned and burned mixtures in terms of in - cylinder temperature and λ (Equation 5 and Equation 6 respectively). The ranges of temperature for the unburned and burned mixtures respectively were 300 K - 1,500 K and 300 K - 2,500 K.

$$\gamma_u = a_1 + a_2T + a_3T^2 + a_4T^3 + a_5T^4 + a_6T^5 + a_7/\lambda \quad (5)$$

$$\gamma_b = b_1 + b_2T + b_3/\lambda + b_4T^2 + b_5/\lambda^2 + b_6T/\lambda + b_7T^3 + b_8/\lambda^3 + b_9T/\lambda^2 + b_{10}T^2/\lambda \quad (6)$$

The final derived equation of γ was expressed as given in Equation 7.

$$\gamma = MFB\gamma_b + (1 - MFB)\gamma_u \quad (7)$$

MFB in Equation 7 represents the Mass Fraction Burned.

The coefficients in Equation 5 and Equation 6 were given by the authors as shown in Table A.1.

Ceviz and Kaymaz [1] used a FIAT, 1.801 dm³ (0.0018 m³), four stroke SI engine to investigate the accuracy of their γ model. The engine was operated at $\frac{3}{4}$ throttle valve opening position and 2,500 rpm at λ values of 0.996, 1.089, 1.216 and 1.341. According to the authors, the proposed γ model was accurate for SI engines when λ was approximately 1.1.

The derived γ model of Ceviz and Kaymaz [1] accounted for important combustion parameters such as temperature and λ . Nonetheless, the model cannot be used as it is for the analysis of the HRR of a CI engine. The authors validated the model using an SI engine operating at near - stoichiometric conditions and a single speed value (2,500 rpm). Modern diesel engines operate by the auto - ignition of compressed, lean air - fuel mixtures. Consequently, the unburned mass fraction in diesels is negligible. Furthermore, CI (diesel) engines operate within a much wider range of λ . For these reasons, the derived equation of Ceviz and Kaymaz [1] was modified in this work by equating *MFB* to 1 so that $\gamma_{mod}(T, \lambda) = \gamma_b$ (Equation 6).

Heywood [9] investigated the dependence of γ on temperature, λ and EGR rate or residual gas composition for a gasoline - air mixture. The results were presented as a graph of γ against temperature for various values of λ and EGR (Figure A.3). However, the γ profiles presented need to be fitted into a mathematical expression so that they can be readily utilized in mathematical modelling. The maximum temperature in the data that is depicted in Figure A.3 is 1,000 K. The combustion temperatures that are obtainable in CI engines are known to be

much higher than 1,000 K. As such, the fitted data of Heywood [9] were extrapolated to values beyond 1,000 K.

The EGR operating limits in stoichiometric SI engines is 20% to 35%. This is because the lowest possible NOx emission occurs within the EGR rate of 20% to 40% as depicted in Figure A.4 [9] for an SI engine at 1,400 rpm and 324 kPa Indicated Mean Effective Pressure (IMEP). Also, moderate - burn and fast - burn SI engine operations have the same NOx emission values within the given EGR operating range. The effect of EGR rate on the HRR model of diesel engines was investigated in this work within the stated EGR operating range (20% to 40%).

2. Methodology

2.1 Model assumptions

The following assumptions were made to develop the HRR model and to carry out the HRR analysis in this work:

- i. Single zone combustion (combustion parameters were uniform in the cylinder).
- ii. A zero - dimensional (transient) HRR model.
- iii. Ideal gas behavior.
- iv. The volume of fuel injected was injected at a temperature of 50 °C and at the pressure of the common rail (160 MPa).
- v. Evaporation of the injected fuel mass was followed by combustion [10].
- vi. The unburned fuel mass was negligible owing to lean combustion and auto - ignition of compressed charge in diesels.

2.2 Leeds CI engine HRR model development

The Leeds HRR model of the engine (Equation 8) was derived from the First Law of thermodynamics. The details of the derivation are given in Appendix B.

$$\frac{dQ}{d\theta} = \frac{\gamma}{\gamma-1} p \frac{dV}{d\theta} + \frac{1}{\gamma-1} V \frac{dp}{d\theta} + \frac{dQ_W}{d\theta} + h_{bb} \frac{dm_{bb}}{d\theta} + q_e \frac{dm_f}{d\theta} \quad (8)$$

$\frac{dQ}{d\theta}$ = rate of release of heat energy from injected fuel, J/deg

p = instantaneous pressure of the cylinder, Pa

V = instantaneous volume of the cylinder, m³

$\frac{dQ_W}{d\theta}$ = heat losses through the walls, J/deg

$\frac{dm_{bb}}{d\theta}$ = blow-by mass flow, kg/deg

h_{bb} = enthalpy of blow-by gases, J/kg

$\frac{dm_f}{d\theta}$ = rate of evaporation of injected fuel, kg/deg

q_e = heat of evaporation of fuel, J/kg

θ = crank angle degree (CAD)

The heat flow to the walls was calculated from Equation 9.

$$Q_w = hA_s(T - T_{ref}) \quad (9)$$

Q_w = wall losses, J/s

h = heat transfer coefficient, W/m² K

A_s = total surface area of heat loss (cylinder liner area, piston surface and cylinder head above piston)

The cylinder temperature on the other hand, was estimated from the ideal gas law (Equation 10)

$$T = pV/mR \quad (10)$$

m = amount of gas in the cylinder, kmol

R = universal gas constant, kJ/kmol K

2.3 Heat transfer coefficient models

Hohenberg's heat transfer correlation (Equation 11) was utilized in this work to calculate the HRR of the engine.

$$h = 130V^{-0.06}p^{0.8}T^{-0.4}(c_m + 1.4)^{0.8} \quad (11)$$

V , p and T are cylinder volume (m³), pressure (Pa) and temperature (K) respectively while c_m is the mean piston speed (m/s).

Fuel injection in CI engines occurs at elevated pressures and at temperatures well above ambient. Therefore, to further enhance the accuracy of the improved HRR model in this work, the equation of Schaschke, Fletcher [11] (Equation 12) was used to correct the density of the injected fuel to the common rail pressure, p of 160 MPa and injection temperature of 50 °C.

$$\rho = 829 + 0.59p - 0.0007p^2 \quad (12)$$

2.4 Engine and instrumentation

The details of the engine, instrumentation and test conditions that were used were as summarized in Tables 1, 2 and 3 below.

Table 1 Engine description

| Feature | Specification |
|-------------|--|
| Type | 4 - stroke, 4 - cylinder compression ignition engine |
| Make | IVECO, EURO V FIAT |
| Rated power | 96 kW |
| Bore/Stroke | 95.8 mm/104 mm (0.0958 m/0.104 m) |

| | |
|-------------------------------------|----------------------------------|
| Compression ratio | 18:1 |
| Fuel | Off - road diesel |
| Injection strategy | Multiple |
| Swept volume per cylinder | 749 cc (0.00075 m ³) |
| Total/effective volume per cylinder | 794 cc (0.0008 m ³) |
| Dynamometer | 100 kW AC Dynamometer |
| Injection pressure | 160 MPa (1,600 bar) |

Table 2 Instrumentation

| Parameter | Equipment specification |
|--------------------|-------------------------------|
| Cylinder pressure | FlexIFEM Indi 601 (2-channel) |
| Fuel flow | Fuel meter (BC 3034) |
| Engine temperature | Thermocouples |

Table 3 Test conditions

| Test | Engine speed, rpm | Torque, Nm |
|------|-------------------|------------------|
| 1 | 1,500 | 30, 75, 150, 220 |
| 2 | 1,600 | 30, 75, 150, 220 |
| 3 | 3,000 | 30, 75, 150, 220 |

2.5 Exponential fit of experimental specific heats data

The experimental data of Heywood [9] (Figure A.1) were fitted into an exponential function (Equation 13) using Mathcad14 software.

$$\gamma = \omega_1 \times \exp(\omega_2 \times T) + \omega_3 \quad (13)$$

The estimated values of the constants ω_1 , ω_2 and ω_3 in Equation 13 were as given in Table B.1 for various values of equivalence ratio, ϕ as well as EGR rate.

Equation 13 was used to model the HRR of the engine at $\phi = 1$ and EGR rates of 0, 0.2 and 0.4 in order to investigate and ascertain the effect of EGR rate on the HRR of the engine.

The input data (pressure traces) that were used to carry out this analysis were presented as shown in Figure B.2 to B.4 in Appendix B.

3. Results and discussions

3.1 Evaluated cylinder temperatures

The cylinder temperatures that were calculated from the measured cylinder pressures and utilized in the HRR analysis were presented graphically as shown in Figures 1 to 3 for the test conditions that were considered.

The temperature profiles indicated that, for each of the engine speeds, the temperature of the flame increased as the load on the engine increased. The peak temperatures for the modes at 1,500 rpm and 1,600 rpm occurred at Degree Crank Angles (CAD) of 21, 25, 33 and 31 for 30 Nm, 75 Nm, 150 Nm and 220 Nm loads respectively. However, the peak temperatures occurred earlier at 21, 22, 22 and 19 CAD respectively for the same torques but at 3,000 rpm. This indicated that, at high engine speed and load, the HRR and peak temperature were higher, and the peak temperature occurred earlier than when the engine was operated at relatively low load conditions.

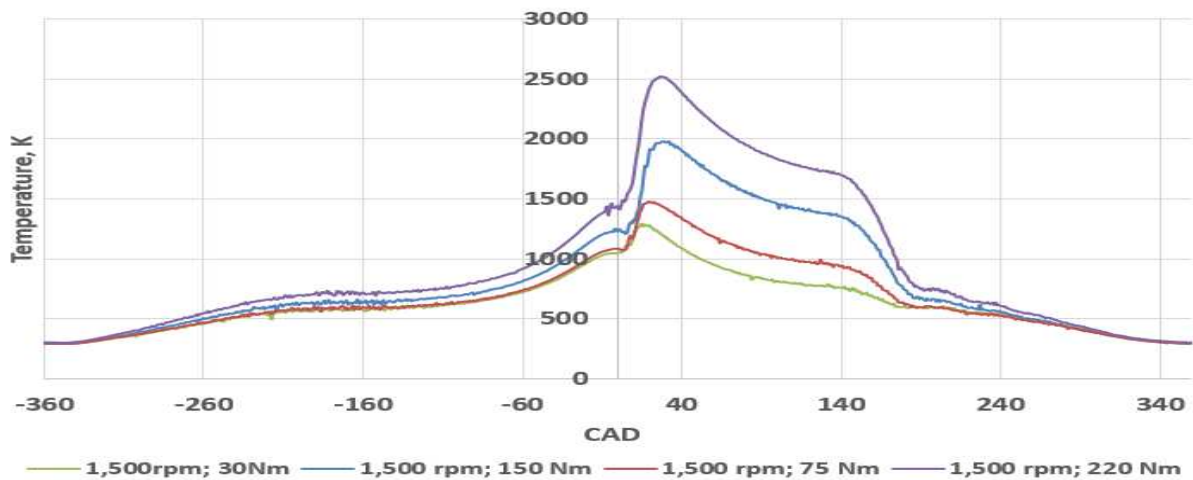


Fig. 1. Calculated in-cylinder temperatures as a function of crank angle with different loads at 1,500 rpm

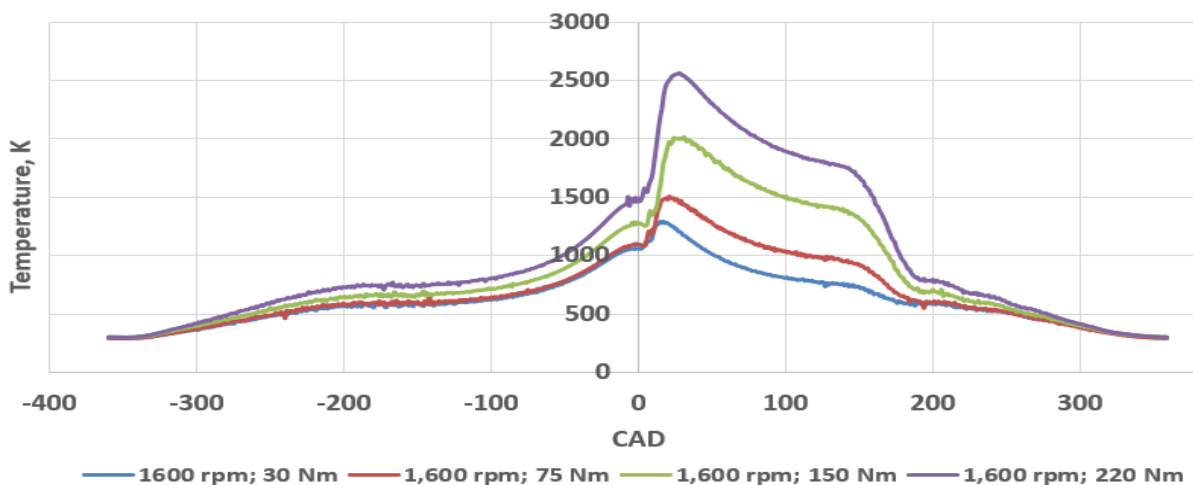


Fig. 2. Calculated in-cylinder temperatures as a function of crank angle with different loads at 1,600 rpm

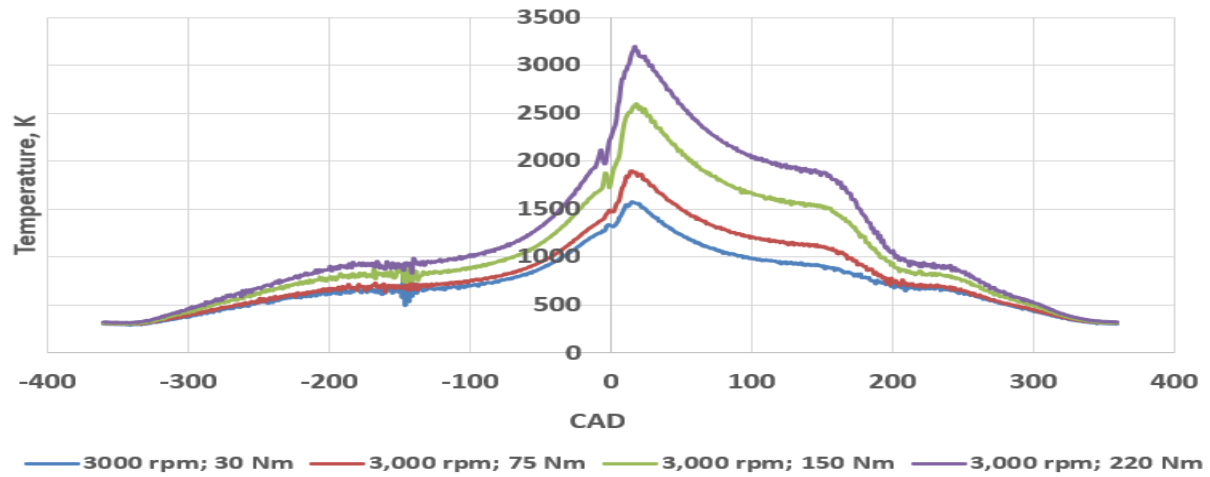


Fig. 3. Calculated in-cylinder temperatures as a function of crank angle with different loads at 3,000 rpm

The observed fluctuations of the temperature profiles near the Top Dead Centre (TDC) in Figure 1, Figure 2, and Figure 3 above were as a result of the auto-ignition of pre-injected fuel with simultaneous injection of fuel. The engine utilized a multiple fuel injection strategy as stated in Table 1. Typically, in the EURO V IVECO engine that was used in this work, fuel injection began before TDC and continued after TDC. The maximum number of injections that occurred in the engine per thermodynamic cycle was eight. (The number of fuel injections per cycle as well as the specific crank angle timing of the injections varied as the speed and the torque of the engine was changed.)

3.2 Effect of EGR rate on engine HRR

Figures 4 to 6 depict the effects of EGR rate on the HRR model of the engine for near-stoichiometric conditions. A near-perfect overlap of the HRR profiles was observed as shown in the figures (except Figure 6) for all the EGR rates that were considered (0, 20% and 40%). It can therefore be inferred that, when $\phi = 1$, for operation at low and medium loads, the effect of EGR rate on the HRR of ICEs is negligible.

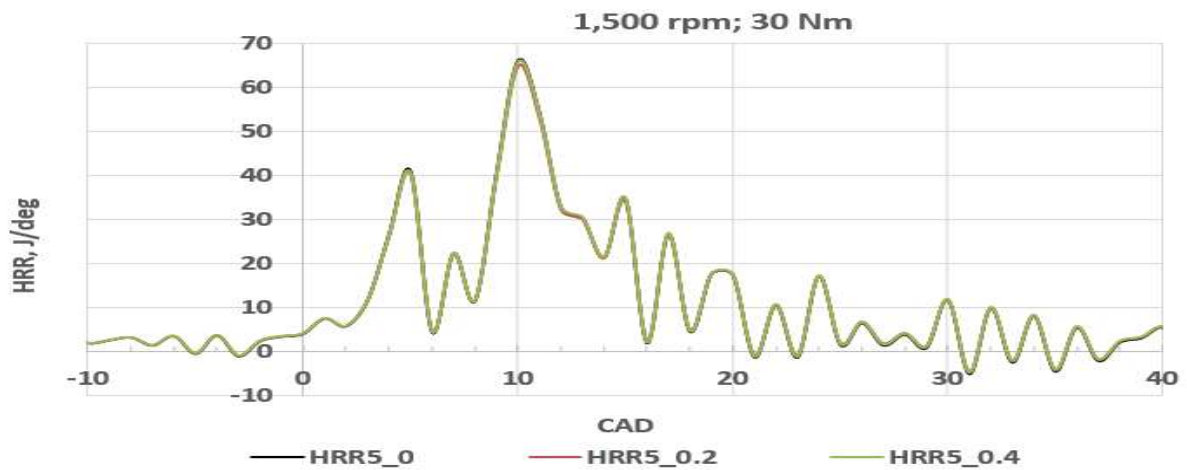


Fig. 4. HRR as a function of EGR rate at 1,500 rpm; 30 Nm

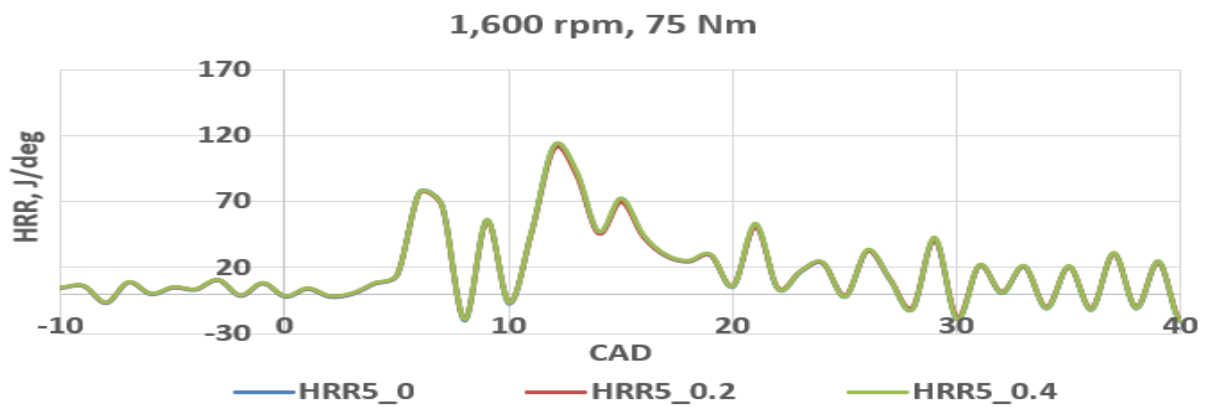


Fig. 5. HRR as a function of EGR rate at 1,600 rpm; 75 Nm

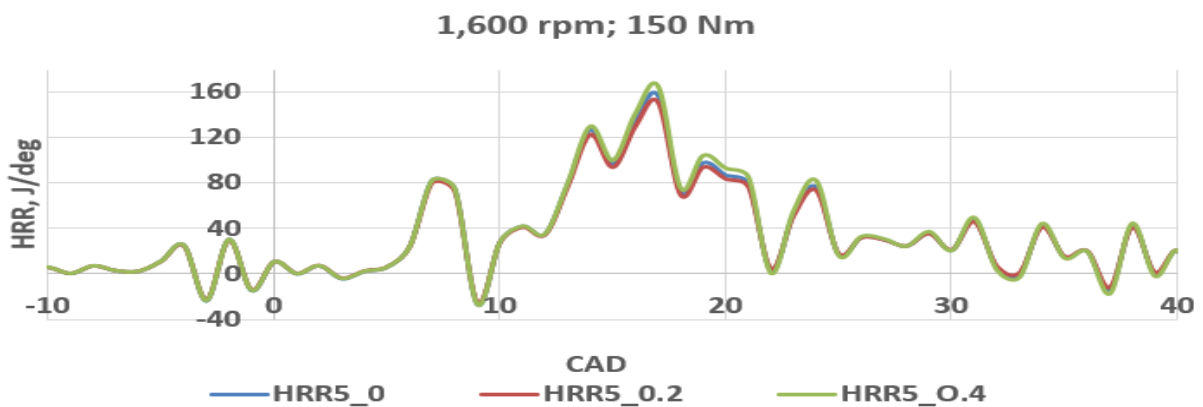


Fig. 6. HRR as a function of EGR at 1,600 rpm; 150 Nm

The graphical comparison of the HRR model that was based on the γ function of Blair [8], HRR4 and the HRR model that was based on the γ model of Heywood [9] at zero EGR rate, HRR5_0 was presented as shown in Figure 7. The model that was based on the γ function of Blair [8] (Equation 7) was chosen for the comparison that was presented in Figure 7 because

Equation 7 is also for a stoichiometric engine without EGR. The PHRR predicted by HRR5_0 (66.19 J/deg) is approximately 8% higher than the value predicted by HRR4 (60.80) for the operation mode (1,500 rpm; 30 Nm). The disparity between the predicted PHRR by HRR4 and HRR5_0 was due to the use of a γ function in HRR5_0 that was derived by fitting and extrapolating experimental data from gasoline – air mixture.

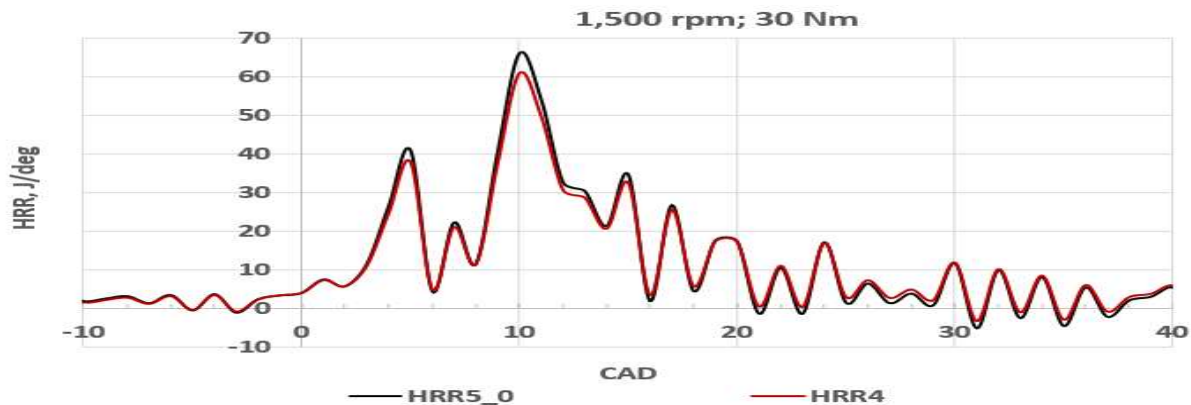


Fig. 7. HRR profiles based on the γ functions of Heywood and Blair

3.3 Comparison of the modified γ function and γ functions from literature

The values of γ estimated from various γ functions were plotted, as depicted in Figure 8, against the temperature of the gases in the cylinder for 1,600 rpm; 30 Nm operation mode. In Figure 8, the values of γ estimated from Equations 1 – 4 that expressed $\gamma(T)$ were graphically compared to the values evaluated using the modified gamma function, γ_{mod} . Gamma 1 - 4 corresponds to the gamma values predicted by Equations 1 – 4 respectively. As shown in Figure 8, the estimated values of γ from γ_{mod} at all temperature points were much higher than the estimates from the other functions which expressed γ as a function of temperature only. Therefore, it can be inferred that λ has a significant effect on γ .

3.4 Effect of λ on γ using the modified γ function.

Figure 9 depicts the dependence of γ on temperature and the excess air ratio, λ . γ in Figure 9 were estimated from γ_{mod} . At temperatures below 1,200 K, γ decreased as temperature increased. However, γ increased as the excess air ratio of the engine increased due to increase in load. Figure 9 clearly showed that γ increased as the combustion became leaner (as λ increased from 2.1 to 8.4).

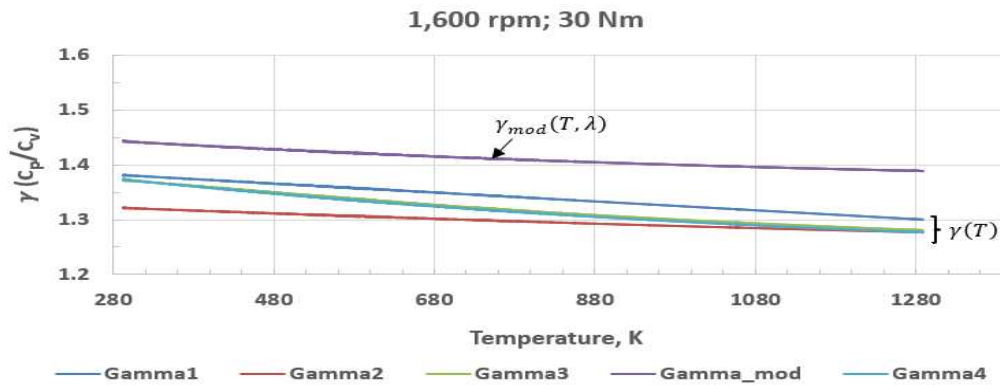


Fig. 8. Comparison of γ_{mod} and γ functions from literature

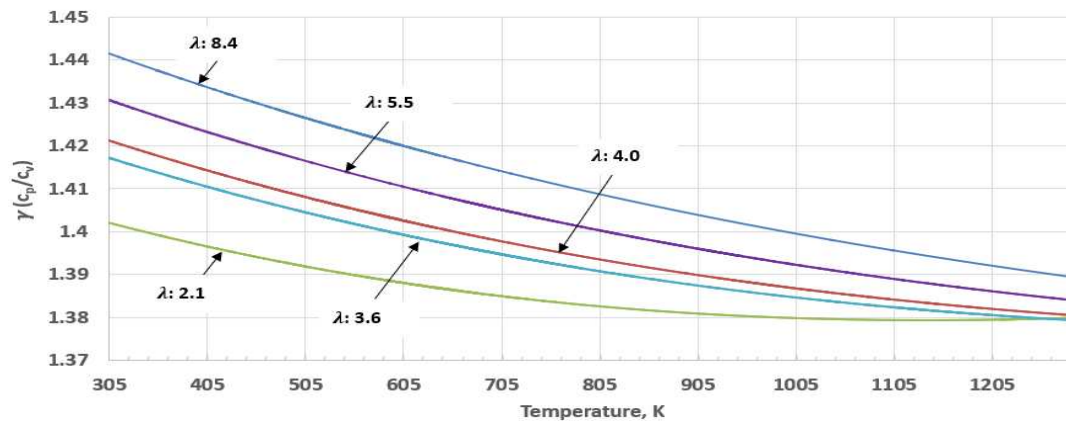


Fig. 9. Variation of γ with λ and temperature as predicted by γ_{mod}

3.5 Sensitivity of engine HRR model to γ functions - comparison of Leeds model to others

The HRR profiles from the investigated HRR models were presented as shown in Figure 10, Figure 11 and Figure 12. The figures clearly showed the sensitivity of the HRR model of the engine to γ functions as the five HRR models predicted different PHRR values. The Leeds HRR model predicted the lowest PHRR for all the modes that were tested. As observed in Figure 8, $\gamma(T, \lambda)$ gave estimates of γ that were higher than the estimates from $\gamma(T)$. However, figures 10 – 12 showed that the HRR model that utilized $\gamma(T, \lambda)$ predicted lower PHRR values for the CI engine than the HRR models that utilized $\gamma(T)$. The five HRR models exhibited the same trend but different PHRR for each of the engine modes that was investigated. Therefore, model validation was carried out by comparing the fuel consumption of the engine predicted by the models to the measured fuel consumption (Section 3.6).

The timing of the PHRR can be determined from the HRR profile. As depicted in Figure 10, the PHRR for the 1,500 rpm; 30 Nm mode occurred at 10° aTDC. Multiple peaks were also observed in the HRR profiles due to multiple fuel injection strategy. The 1,500 rpm; 75 Nm engine mode showed two prominent peaks. Peak_1 was as a result of the heat released from the combustion of the fuel that was injected during pilot fuel injection. There was a main injection event at 6° aTDC which caused another ignition and heat release leading to Peak_2.

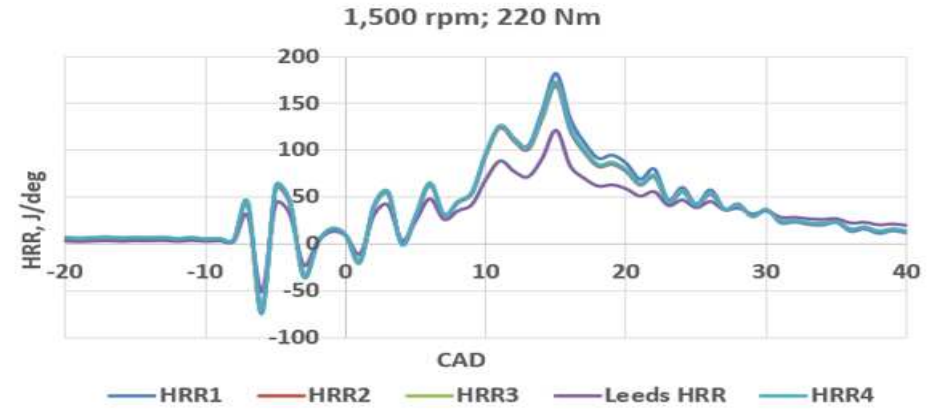
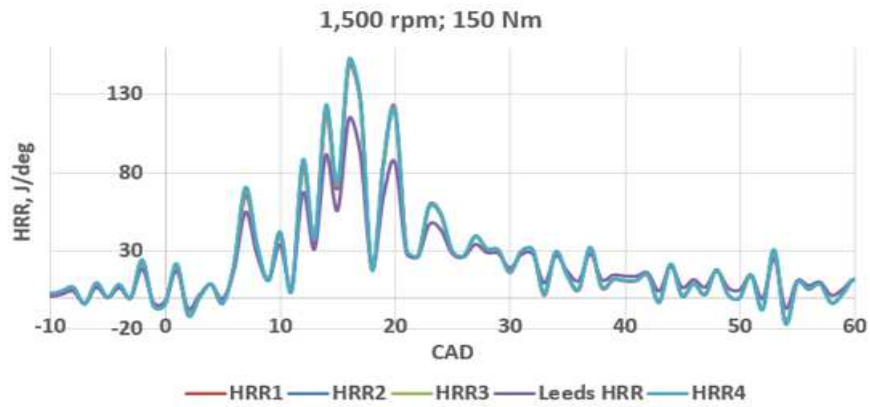
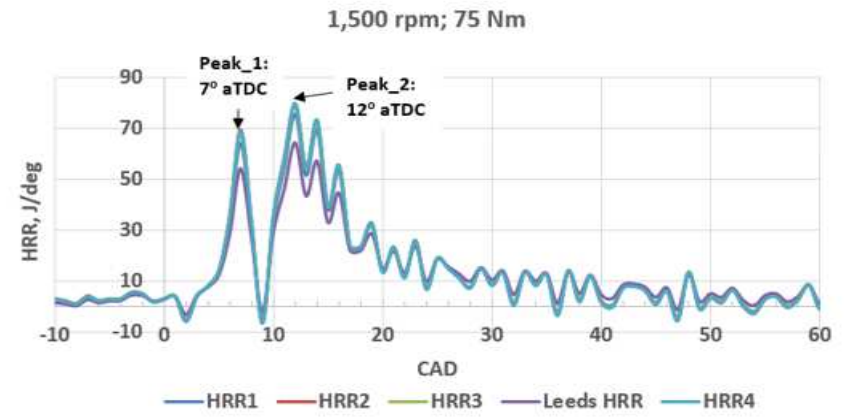
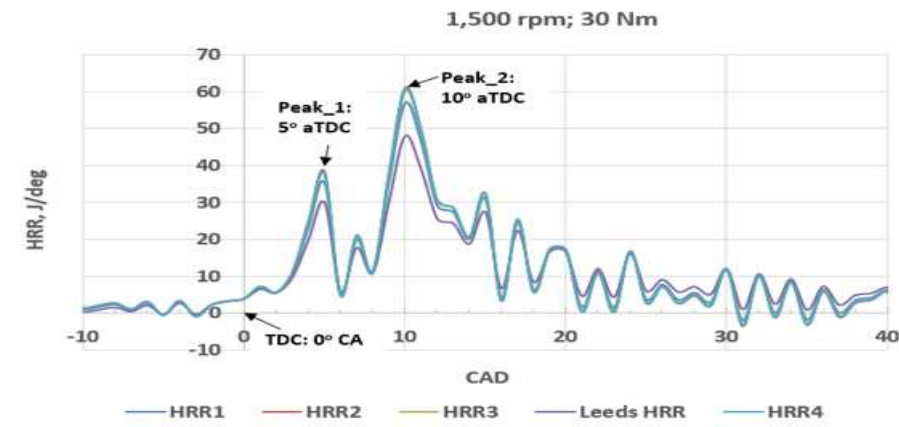


Fig. 10. HRR profiles from the Leeds model and other models (1,500 rpm modes)

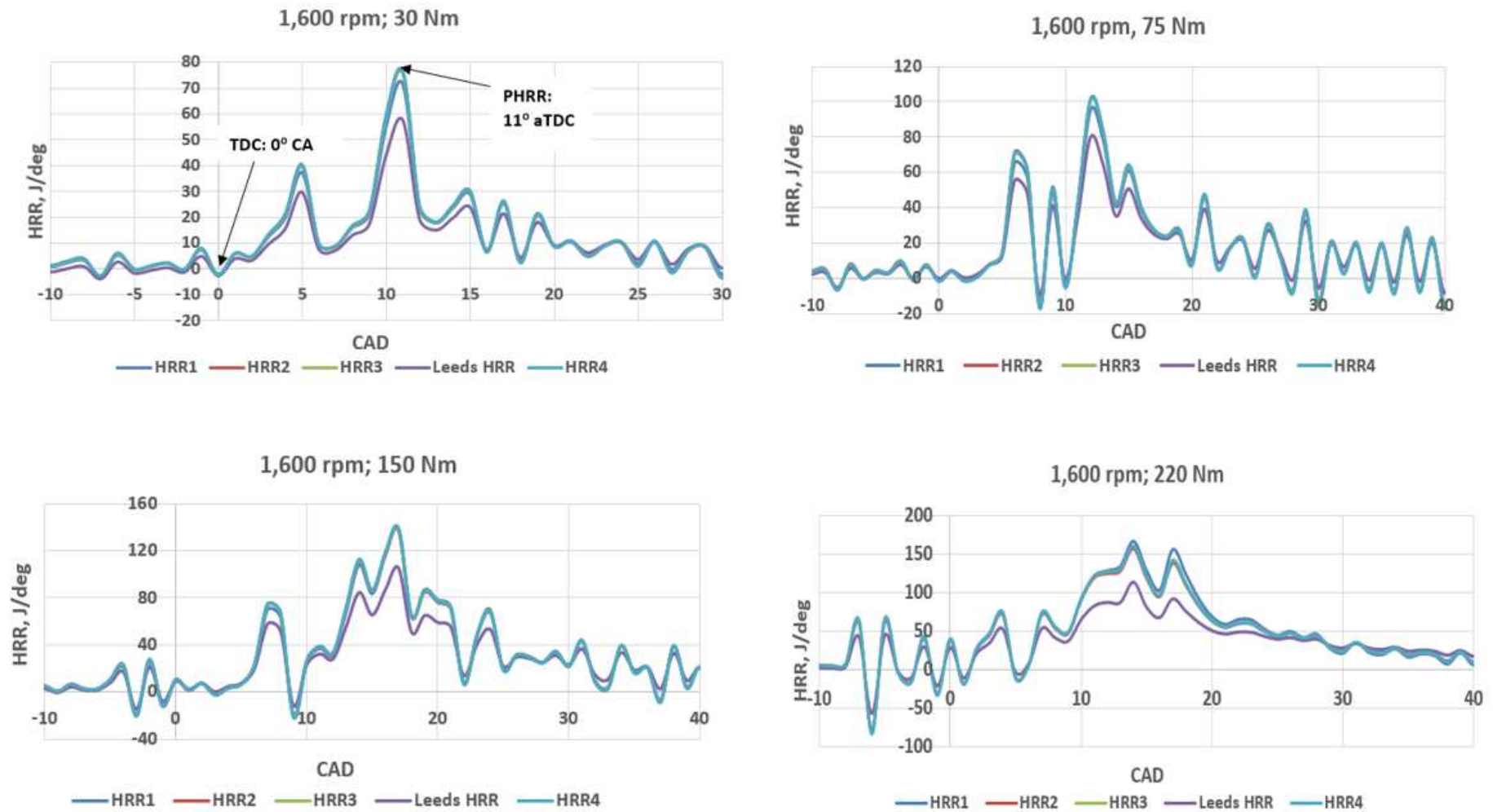


Fig. 11. HRR profiles from the Leeds model and other models (1,600 rpm modes)

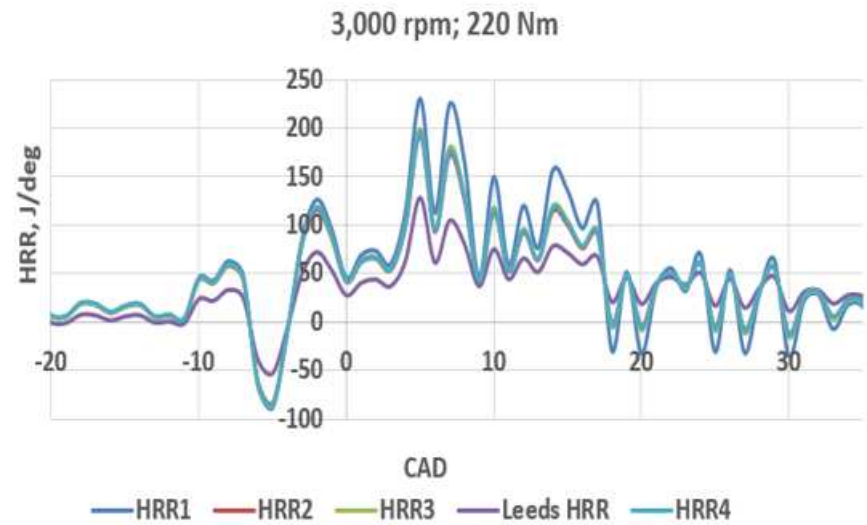
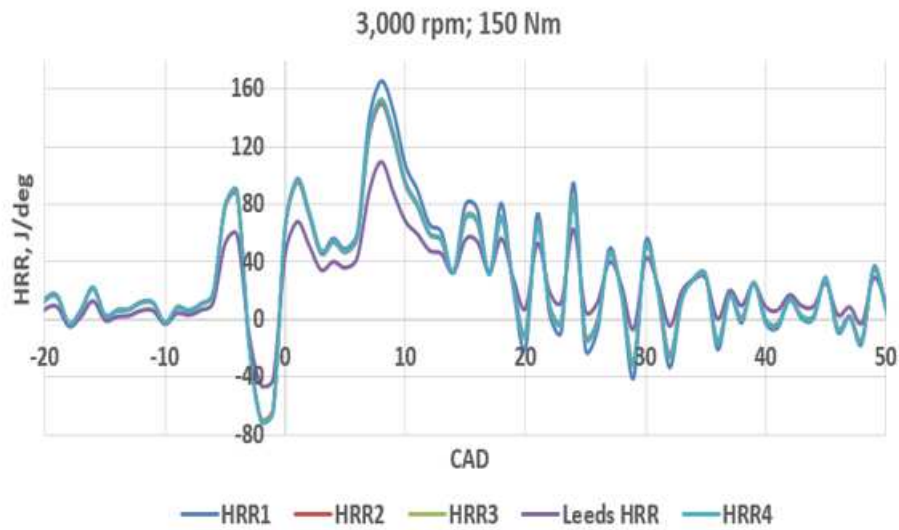
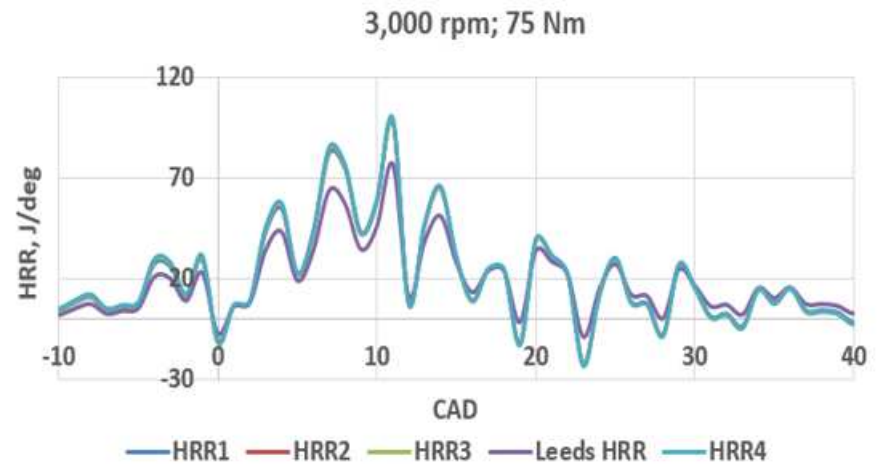
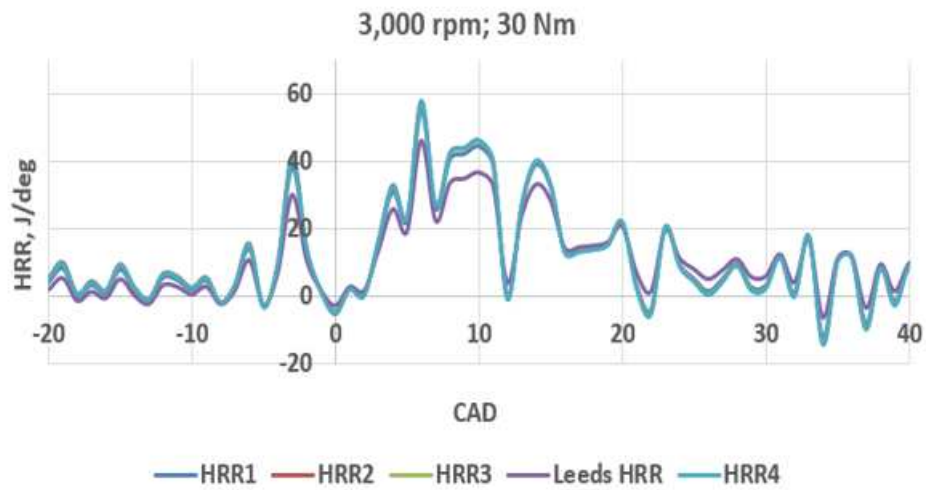


Fig. 12. HRR profiles from the Leeds model and other models (3,000 rpm modes)

3.6 Leeds model validation

The fuel consumption of the engine per thermodynamic cycle per cylinder was estimated from the Cumulative Heat Release (CHR) profiles obtained from the five HRR models. The CHR profiles based on Leeds HRR model, (strictly for the heat that was released as a result of the combustion of injected fuel) were as depicted in Figure 13, Figure 14, and Figure 15. The figures present the heat that was released in each of the four cylinders per power stroke (in joules) from the combustion of the injected fuel mass.

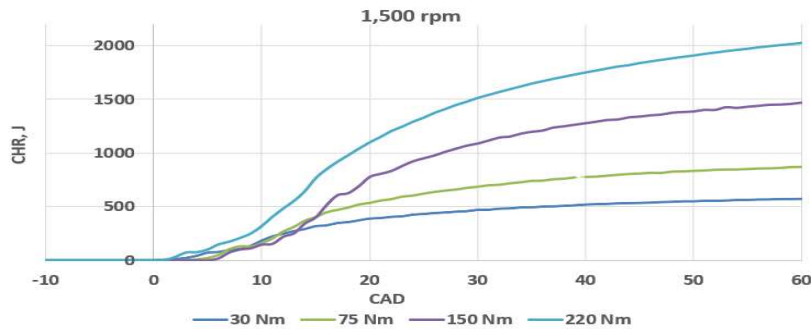


Fig. 13. Cumulative heat release profiles (1,500 rpm modes)

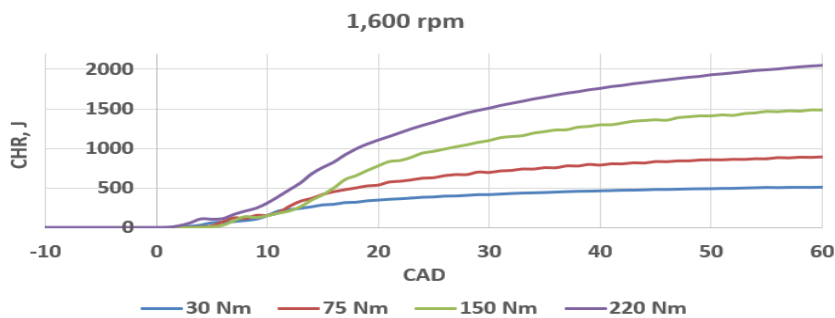


Fig. 14. Cumulative heat release profiles (1,600 rpm modes)

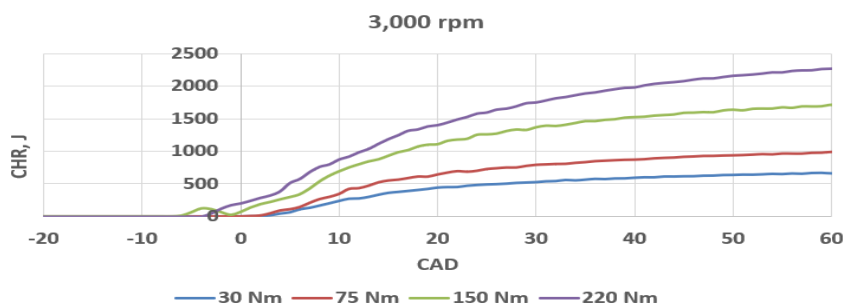


Fig. 15. Cumulative heat release profiles (3,000 rpm modes)

The result of the validation of the HRR models were presented graphically as shown in Figure 16. Figure 16 showed that the fuel masses predicted by the Leeds model (the pink bars) for all the engine modes were the most accurate. The Leeds HRR model that was based on the

modified γ function, $\gamma_{mod}(T, \lambda)$, predicted the fuel consumption of the engine with an average (absolute) error of 1.41% compared to the measured fuel consumption. The percentage errors of the fuel masses predicted by the Leeds HRR model ranged from -3.68 to +4.08, with a standard deviation of 1.21. The average error in the predicted fuel masses by the other HRR models that were based on $\gamma(T)$ ranged from 15.85% to 16.36%. The HRR models that were based on $\gamma(T)$ overpredicted the fuel consumption of the engine because the significant effect of λ on γ was neglected in the models. Figure 16 clearly showed that the accuracy of the HRR model of CI engines is enhanced by using $\gamma(T, \lambda)$ at both near – stoichiometric and non-stoichiometric operating conditions.

The analysis that was done to compare the predicted fuel masses to the measured fuel mass was summarized as presented in Table C.1.

3.7 Determination of combustion phasing

The validated model (Leeds model) was used to determine the SoC, EoC and the crank angle timing at which 50% of the injected fuel mass was burned (MFB50) from the fuel burn profiles of the modes that were tested. The phasing of the combustion (SoC, MFB50, EoC) for the 1,500 rpm; 150 Nm test mode was determined as shown in Figure 17. The figure showed that, when the engine was run at 1,500 rpm and 150 Nm, the SoC was at 5° aTDC, 50% of the injected fuel was burned at 19° aTDC while the EoC was at 51° aTDC. The phasing of the combustion for the other modes was determined in a similar manner and tabulated as shown in Table 4.

Table 4 Combustion phasing of the tested engine modes

| Engine speed, rpm | Torque, Nm | SoC, CAD | EoC, CAD | MFB50, CAD |
|-------------------|------------|----------|----------|------------|
| 1,500 | 30 | 0 | 18 | 10 |
| | 75 | 3 | 35 | 14 |
| | 150 | 5 | 51 | 19 |
| | 220 | 2 | 60 | 18.5 |
| 1,600 | 30 | 1 | 21 | 10.5 |
| | 75 | 2 | 33 | 14 |
| | 150 | 3 | 45 | 18.5 |
| | 220 | 2 | 55 | 18 |
| 3,000 | 30 | 0 | 33 | 12 |
| | 75 | 1 | 47 | 13 |
| | 150 | -1 | 35 | 10.5 |
| | 220 | -5 | 47 | 13 |

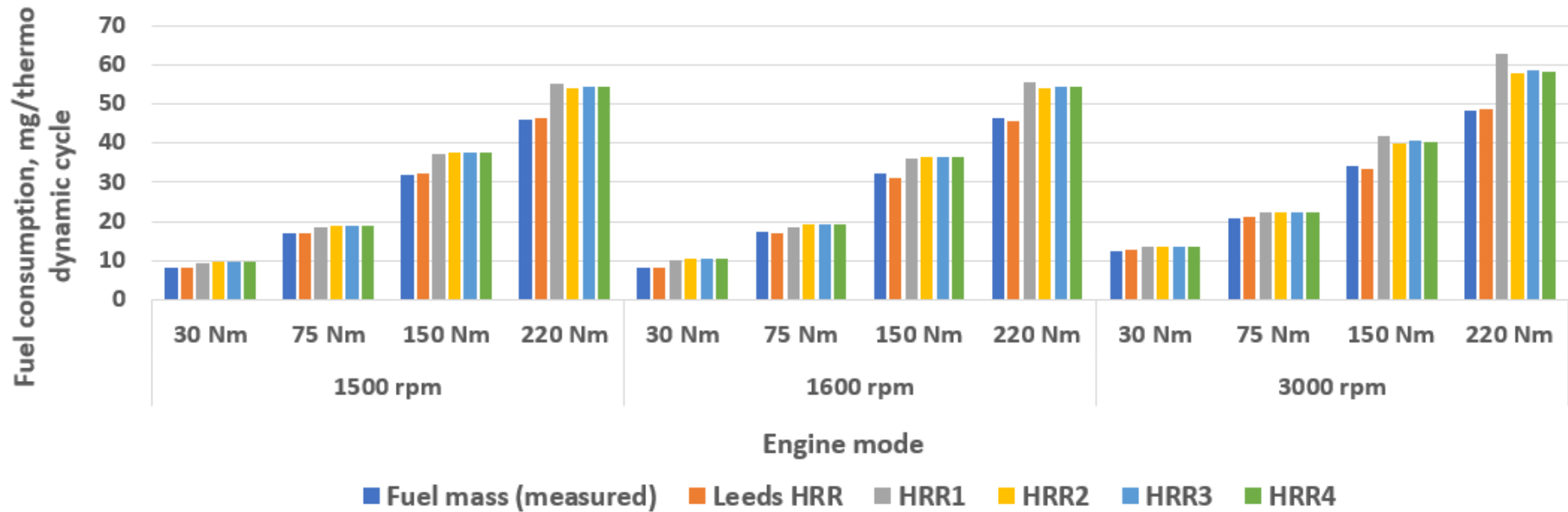


Fig. 16. Comparison of measured and predicted fuel masses

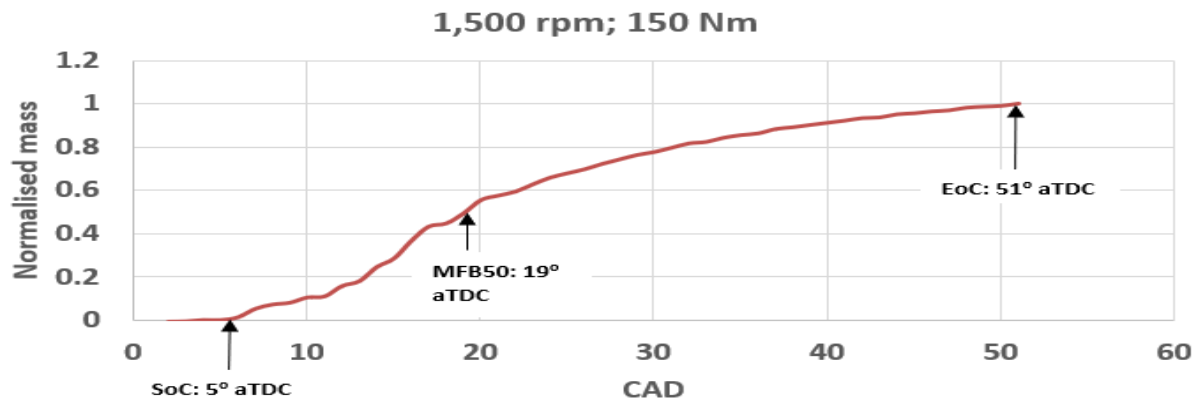


Fig. 17. Determination of combustion phasing from fuel burn profile

4. Conclusions

In this work, an improved HRR model – Leeds HRR model - was developed for the analysis of the HRR of a multiple fuel injection, CI (diesel) engine operated at non – stoichiometric conditions ($\lambda > 1$). No work has been done in the past to develop a mathematical model for the analysis of the HRR of diesel engines within a wide range of non – stoichiometric conditions. The current work has shown that the accuracy of the HRR models of CI engines is strongly depended on the specific heats ratio (γ). Most of the existing HRR models were based on $\gamma(T)$. The effect of the excess air ratio (λ) on γ was investigated in this work. λ was found to have a significant effect on γ . Therefore, in the current work, a modified γ function, $\gamma_{mod}(T, \lambda)$ was used to model the HRR of the engine, i.e. the Leeds HRR model. The Leeds HRR model based on $\gamma_{mod}(T, \lambda)$ predicted the fuel consumption of the engine with an average (absolute) error of 1.41%. The errors in the fuel masses predicted by the Leeds HRR model ranged from -3.68% to +4.08%, with a standard deviation of 1.21. The average error in the fuel mass predictions of the other models which were based on $\gamma(T)$ ranged from 15.85% to 16.36%. The error in the prediction of the other models was largely because λ was neglected in the models. Therefore, in this work, it was shown that the accuracy of the HRR model of CI engines is enhanced by using $\gamma(T, \lambda)$. The effect of EGR rate on the HRR model of the engine was also investigated in this work using a γ model that was derived from experimental data. It was found that at stoichiometric condition, EGR rate had insignificant effect on the accuracy of the HRR model of the engine specifically for operation at low and medium loads. In the future, the engine will be run on biofuel blends and the validated HRR model will be used to investigate and optimize the combustion behaviour of the fuel blends.

Acknowledgement

This work was supported by the Petroleum Technology Development Fund (PTDF), Nigeria and the National Agency for Science and Engineering Infrastructure (NASeni), Nigeria.

Appendix A

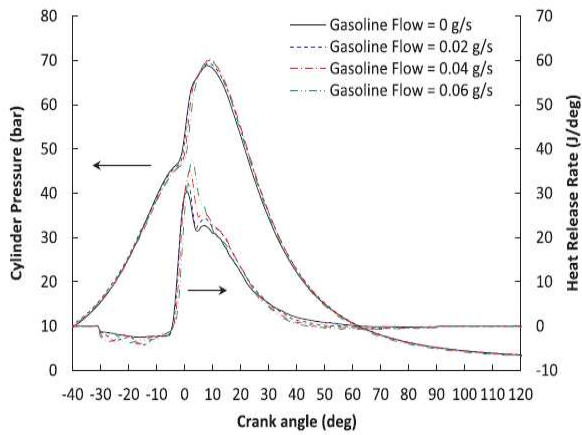


Fig. A.1. Single fuel injection strategy

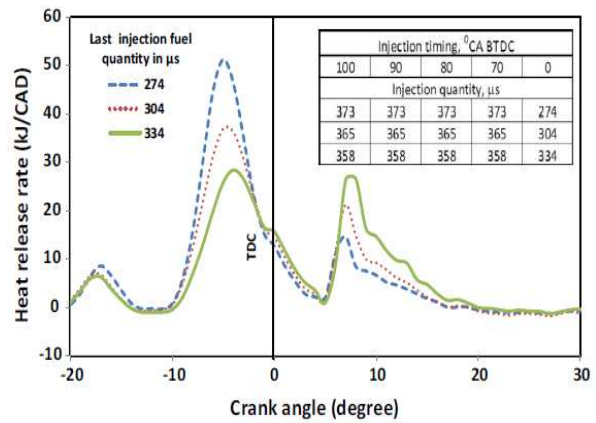


Fig. A.2. Multiple fuel injection strategy

Table A.1 Coefficients for use in the gamma functions of Ceviz and Kaymaz [1]

| Coefficients (γ_u) | Values | Coefficients (γ_b) | Values |
|-----------------------------|--------------|-----------------------------|-------------|
| a_1 | 1.464202464 | b_1 | 1.498119965 |
| a_2 | -0.000150666 | b_2 | -0.00011303 |
| a_3 | -7.34852e-08 | b_3 | -0.26688898 |
| a_4 | 1.55726e-10 | b_4 | 4.03642e-08 |
| a_5 | -7.6951e-14 | b_5 | 0.273428364 |
| a_6 | 1.19535e-17 | b_6 | 5.7462e-05 |
| a_7 | -0.063115275 | b_7 | -7.2026e-12 |
| | | b_8 | -0.08218813 |
| | | b_9 | -1.3029e-05 |
| | | b_{10} | 2.35732e-08 |

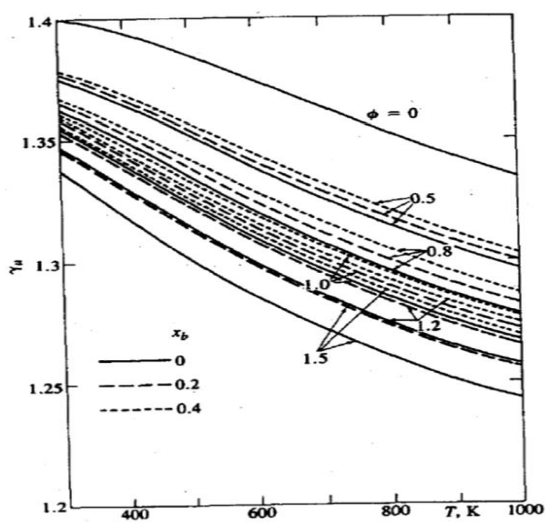


Fig. A.3. EGR dependence of gamma

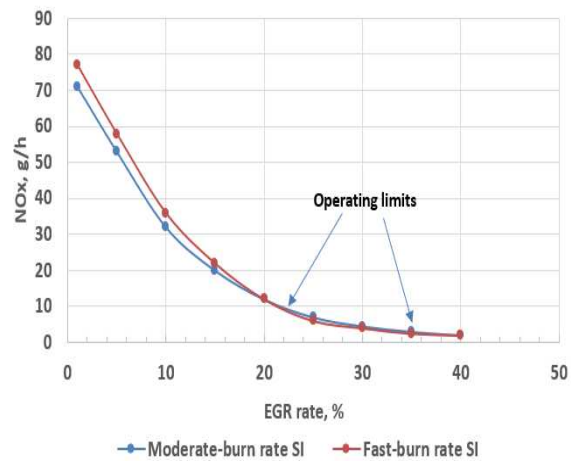


Fig. A.4. EGR operating limits

Appendix B

Modelling of the HRR of CI engine from the first law of thermodynamics

Figure B.1 was used to develop the Leeds HRR model in this work. The energy conversions, transfer and losses that occur in the cylinder of a CI engine during the power stroke are depicted in Figure B.1. A fraction of the heat that is released (dQ) from the combustion of injected fuel in the cylinder is lost through the walls of the cylinder (dQ_w), through the gap between the piston and the cylinder liner by blow-by gases (dQ_b) and as heat retained to increase the internal energy of the gas in the cylinder. The remaining heat is converted to pV (piston) work (pdV). The heat that is lost via blow-by gases, dQ_b is the product of the enthalpy of the blow-by gases, h_{bb} and the mass, dm_{bb} .

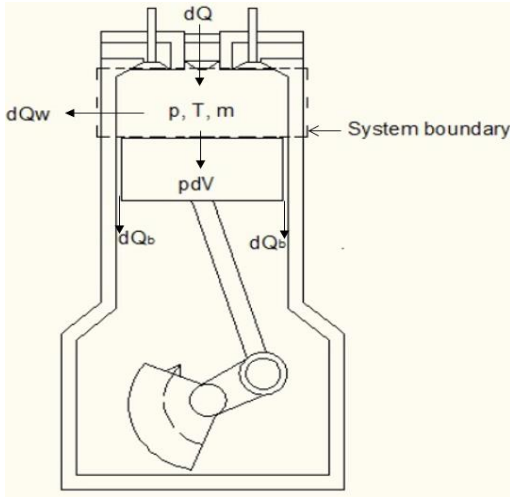


Fig. B.1. Power stroke of a CI engine

B.1 HRR model formulation

The first law of thermodynamics was expressed as given in Equation B.1 for the period between intake valve closing (IVC) and exhaust valve closing (EVC) of engine. The mass in the system boundary (Figure B.1) was assumed constant during this period.

$$\frac{dU}{d\theta} = \frac{dQ}{d\theta} - \frac{dW}{d\theta} - \frac{dQ_w}{d\theta} - h_{bb} \frac{dm_{bb}}{d\theta} - q_e \frac{dm_f}{d\theta} \quad (\text{B.1})$$

$\frac{dU}{d\theta}$ = rate of change of the internal energy of cylinder content

$\frac{dQ}{d\theta}$ = rate of release of heat energy from injected fuel

$\frac{dW}{d\theta}$ = pV work due to piston motion

$\frac{dQ_w}{d\theta}$ = heat losses through the walls

$\frac{dm_{bb}}{d\theta}$ = blow-by mass flow

h_{bb} = enthalpy of blow-by gases

$\frac{dm_f}{d\theta}$ = rate of evaporation of injected fuel

q_e = heat of evaporation of fuel

θ = degree crank angle (CAD)

The pressure-volume work and the change in internal energy were rewritten as in Equation B.2 and Equation B.3 respectively.

$$dW = pdV \quad (B.2)$$

$$dU = mc_v dT \quad (B.3)$$

m = amount of gas in the cylinder, kmol

c_v = specific heat capacity at constant volume, kJ/kmol K and T = temperature, K

The ideal gas law was expressed as:

$$dT = d(pV)/mR \quad (B.4)$$

R = universal gas constant, kJ/kmol K

Equation B.5 was used to express the relationship between R , γ and c_v .

$$R/c_v = \gamma - 1 \quad (B.5)$$

The final HRR model; Leeds HRR model, (Equation B.6) was obtained by substituting Equations B.2 – B.5 into Equation B.1 and rearranging.

$$\frac{dQ}{d\theta} = \frac{\gamma}{\gamma-1} p \frac{dV}{d\theta} + \frac{1}{\gamma-1} V \frac{dp}{d\theta} + \frac{dQ_W}{d\theta} + h_{bb} \frac{dm_{bb}}{d\theta} + q_e \frac{dm_f}{d\theta} \quad (B.6)$$

Table B.1 Constants to be used in the derived (fitted) model of γ

| Equivalence ratio, ϕ | EGR | ω_1 | ω_2 | ω_3 |
|---------------------------|-----|------------|------------|------------|
| 0.5 | 0.4 | 0.429 | -0.00031 | 0.988 |
| 0.8 | 0.2 | 0.412 | -0.00038 | 0.997 |
| 0.8 | 0.4 | 0.358 | -0.00044 | 1.054 |
| 1 | 0 | 0.241 | -0.00092 | 1.172 |
| 1 | 0.2 | 0.223 | -0.00105 | 1.195 |
| 1 | 0.4 | 0.384 | -0.00042 | 1.022 |

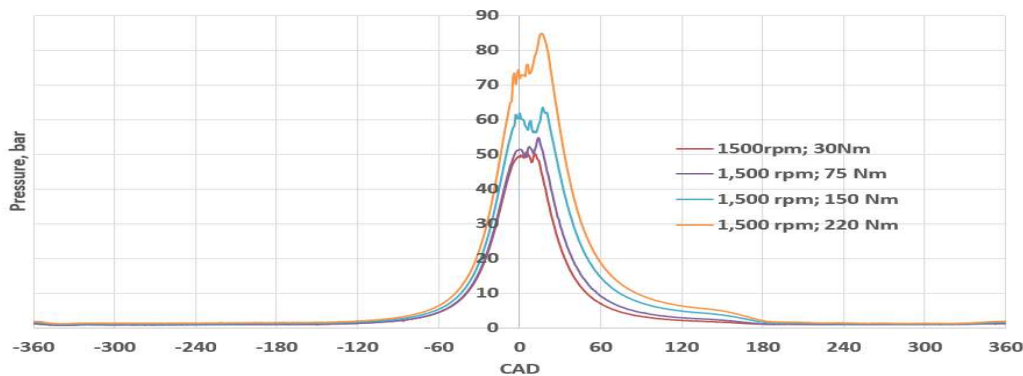


Fig. B.2. Pressure trace (1,500 rpm modes)

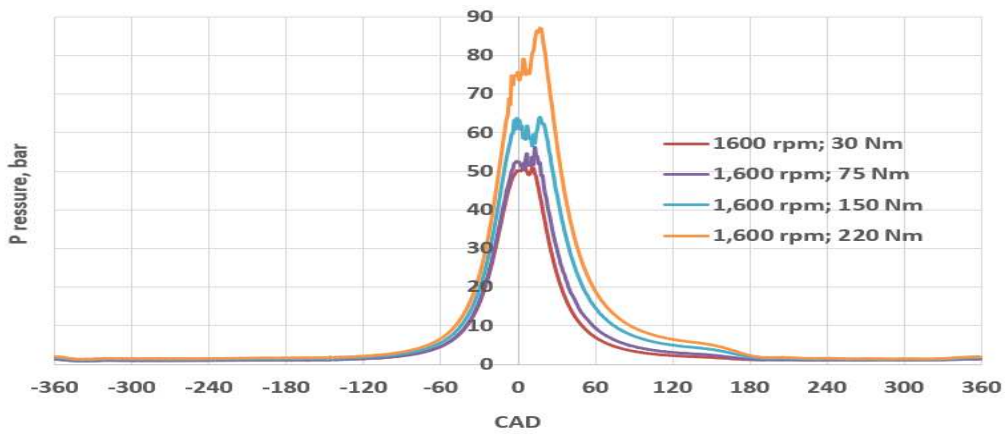


Fig. B.3. Pressure trace (1,600 rpm modes)

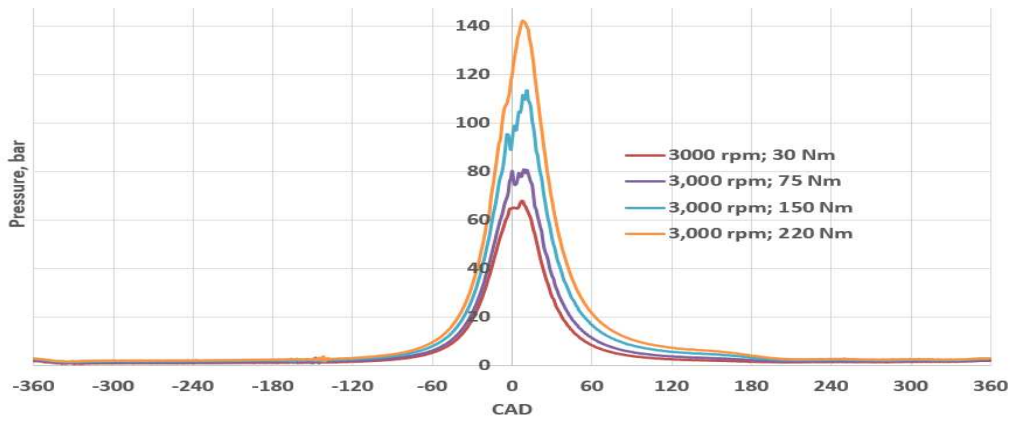


Fig. B.4. Pressure trace (3,000 rpm modes)

Appendix C
Summary of analysis of model results

Table C.1 Model validation

| Engine speed, rpm | Torque, Nm | Lambda, λ | Fuel mass, mg/thermodynamic cycle | | | | | | % Deviation from measured fuel mass | | | | |
|-----------------------------|------------|-------------------|-----------------------------------|-----------|-------|-------|-------|-------|-------------------------------------|--------------|--------------|--------------|--------------|
| | | | Measured | Leeds HRR | HRR1 | HRR2 | HRR3 | HRR4 | Leeds HRR | HRR1 | HRR2 | HRR3 | HRR4 |
| 1,500 | 30 | 8.40 | 8.11 | 8.20 | 9.23 | 9.73 | 9.62 | 9.69 | 1.09 | 13.81 | 19.98 | 18.62 | 19.48 |
| | 75 | 4.04 | 16.87 | 16.84 | 18.41 | 19.05 | 18.95 | 19.06 | -0.21 | 9.11 | 12.93 | 12.32 | 12.97 |
| | 150 | 2.14 | 31.77 | 32.08 | 37.11 | 37.48 | 37.57 | 37.71 | 0.98 | 16.82 | 17.99 | 18.24 | 18.69 |
| | 220 | 1.46 | 46.02 | 46.18 | 55.1 | 54.15 | 54.52 | 54.51 | 0.35 | 19.73 | 17.67 | 18.47 | 18.45 |
| 1,600 | 30 | 8.35 | 8.17 | 8.15 | 9.95 | 10.42 | 10.32 | 10.39 | -0.20 | 21.78 | 27.51 | 26.30 | 27.13 |
| | 75 | 3.97 | 17.18 | 16.87 | 18.59 | 19.22 | 19.14 | 19.25 | -1.8 | 8.23 | 11.87 | 11.39 | 12.06 |
| | 150 | 2.10 | 32.33 | 31.14 | 36.02 | 36.29 | 36.42 | 36.56 | -3.68 | 11.41 | 12.25 | 12.65 | 13.08 |
| | 220 | 1.45 | 46.35 | 45.63 | 55.44 | 54.05 | 54.50 | 54.44 | -1.55 | 19.61 | 16.61 | 17.58 | 17.45 |
| 3,000 | 30 | 5.49 | 12.23 | 12.73 | 13.41 | 13.57 | 13.56 | 13.60 | 4.08 | 9.61 | 10.93 | 10.88 | 11.19 |
| | 75 | 3.56 | 20.97 | 21.21 | 22.28 | 22.28 | 22.32 | 22.35 | 1.16 | 6.23 | 6.25 | 6.45 | 6.57 |
| | 150 | 2.16 | 33.96 | 33.58 | 41.92 | 40.01 | 40.50 | 40.35 | -1.13 | 23.45 | 17.81 | 19.27 | 18.80 |
| | 220 | 1.53 | 48.21 | 48.54 | 62.88 | 57.64 | 58.54 | 58.08 | 0.68 | 30.44 | 19.56 | 21.43 | 20.47 |
| Average of absolute errors: | | | | | | | | | 1.41 | 15.85 | 15.95 | 16.13 | 16.36 |
| Standard deviation: | | | | | | | | | 1.21 | 7.04 | 5.26 | 5.24 | 5.19 |
| Error range: | | | | | | | | | -3.68 - +4.08 | 6.23 - 30.44 | 6.25 - 27.51 | 6.45 - 26.30 | 6.57 - 27.13 |

References

- [1] Ceviz, M.A. and İ. Kaymaz, *Temperature and air–fuel ratio dependent specific heat ratio functions for lean burned and unburned mixture*. Energy Conversion and Management, 2005. **46**(15): p. 2387-2404.
- [2] Wu, A., S. Keum, and V. Sick, *Large eddy simulations with Conjugate Heat Transfer (CHT) modelling of Internal Combustion Engines (ICEs)*. IFP Energies nouvelles, 2019. **74**(51).
- [3] Vipavanich, C., S. Chuepeng, and S. Skullong, *Heat release analysis and thermal efficiency of a single cylinder diesel dual fuel engine with gasoline port injection*. Case Studies in Thermal Engineering, 2018. **12**: p. 143-148.
- [4] Mathivanan, K., J.M. Mallikarjuna, and A. Ramesh, *Influence of multiple fuel injection strategies on performance and combustion characteristics of a diesel fuelled HCCI engine – An experimental investigation*. Experimental Thermal and Fluid Science, 2016. **77**: p. 337-346.
- [5] Gatowski, J.A., et al., *Heat Release Analysis of Engine Pressure Data*. 1984, SAE International.
- [6] Brunt, M.F.J. and A.L. Emtage, *Evaluation of Burn Rate Routines and Analysis Errors*. 1997, SAE International.
- [7] Egnell, R., *Combustion Diagnostics by Means of Multizone Heat Release Analysis and NO Calculation*. 1998, SAE International.
- [8] Blair, G.P., *The basic design of two-stroke engines*. 1990: Warrendale, PA (United States); Society of Automotive Engineers; None. Medium: X; Size: Pages: (692 p).
- [9] Heywood, J.B., *Internal combustion engine fundamentals*. 1988, New York: McGraw-Hill, Inc.
- [10] AVL, *GCA Gas exchange and combustion analysis*. 2015, Germany: AVL.
- [11] Schaschke, C., I. Fletcher, and N. Glen, *Density and Viscosity Measurement of Diesel Fuels at Combined High Pressure and Elevated Temperature*. Processes, 2013. **1**(2): p. 30-48.